A preliminary study of subcooled flow boiling critical heat flux on Cr-coated Zr-based tube for accident-tolerant fuel cladding application

Namgook Kim [a], Hong Hyun Son [a], Sung Joong Kim [a, b*]
[a]*Hanyang University, 222 Wangsimri-ro, Seongdong-gu, Seoul 04763, Republic of Korea*
[b]*Institute of Nano Science & Technology, Hanyang University*
[*]*Corresponding author: sungjkim@hanyang.ac.*

1. Introduction

In development of accident-tolerant fuel (ATF) cladding, surface coating techniques applicable for existing zirconium-based alloys has been issued due to its positive characteristics such as high neutron efficiency and short developing time. In addition, coating process can contribute to additional benefit to enhance boiling heat transfer such as critical heat flux (CHF) [1-2]. Because coating process forms micro/nanoscale structures, which amplifies capillary wicking that plays a key role in enhancing CHF.
In this regard, aim of this study was to evaluate effect of modified surface structures by ATF coating process on flow boiling performance.

2. Experiment

2.1 Sample preparation and surface morphology

The test tubes were prepared following 3 steps of the fabrication; grinding, cleaning and deposition processes. Firstly, we ground the surface of tubes with the same grade of sandpaper because it is widely known that the surface roughness could strongly affect CHF [4]. In the next step, we cleaned the tube in an ethanol during 5 min. and a deionized water during 5 min. using an ultrasonic cleaner. The above 2 steps are also the preparation procedure for bare tube. After the steps, we deposited an ATF candidate material on base material (Zr-based alloy tube) using DC magnetron sputtering technique. In this paper, Chromium (Cr) was selected as a target material for a coating. The selected coating conditions for the purpose of forming a nanoscale surface structures based on a structure zone model [3] were listed in Table I.

Table I: Sputtering conditions for DC magnetron sputtering

Sputtering conditions	Characteristics
Exposure environment	99.95% pure Cr
Substrate temperature (°C)	150
Exposure time (hr)	1
Working pressure (torr.)	1×10^{-2}
DC power (W)	150-160
Sputtering gas	100% Ar

The surface morphology of the fabricated tubes were analyzed using Apreo S Hivac as shown in Fig. 1(a) and (b). There were uni-directional microscale scratches from the initial grinding process on both tubes. On the Cr-coated tube, however, the numerous dome-shaped particulate nanostructures in nanoscale were formed on the top of Cr-coated layer (inset images). Fig. 1(c) and (d) show the cross-sectional SEM images of the fabricated tubes with the milling process using an auto-polisher. It was confirmed that the thickness of Cr-coated layer was approximately 1.0 μm with no significant defection in fine columnar grains.

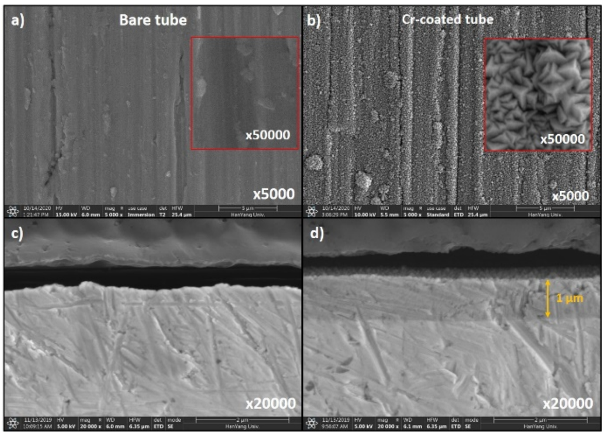

Fig. 1. SEM images of surface morphology on (a) bare tube and (b) Cr-coated tube and cross-sectional images (c) before and (d) after deposition of Cr layer.

2.2 Flow boiling experiment setup

Fig. 2(a) shows a schematic of the forced convective flow boiling test loop. The flow boiling test loop consists of a test section, a boiling chamber, a circulation pump, an accumulator, a preheater, a buffer tank, a shell & tube type condenser, and a shell & tube type heat exchanger. Deionized water, which is used as a working fluid, from a buffer tank is penetrated through a heat exchanger and pumped by a high-temperature centrifugal pump with a maximum operating temperature of 180 °C. The coolant is heated in a preheater with a maximum output power of 20 kW, flows through the inside of the boiling chamber, and is stored again in the buffer tank. The data acquisition system records the flow rate, the pressure, the voltage and the temperature history measured at each component. The flow inside the boiler chamber forms an annular flow through a 20 mm diameter PC tube.
A detailed design of the test section used in the study is shown in Fig. 2(b). The dimension of the test specimen is 3/8 in. diameter and 100 mm length. The heated length is 80 mm because the remaining 10 mm length of both sides is connected with copper electrodes in order to

secure the sufficient electrical contact. The electrical resistance of Zr-based tube was measured to 1.0 mΩ which is much higher than copper resistance of 0.0136 mΩ. The inside of the test tube is insulated by a ceramic-type wool. Three K-type thermocouples are attached inside the tube at a height of 25, 50, and 75 mm to measure an inner wall temperature at each height. Pt wires are connected to both ends of the copper electrode rod along which the voltage drop is measured.

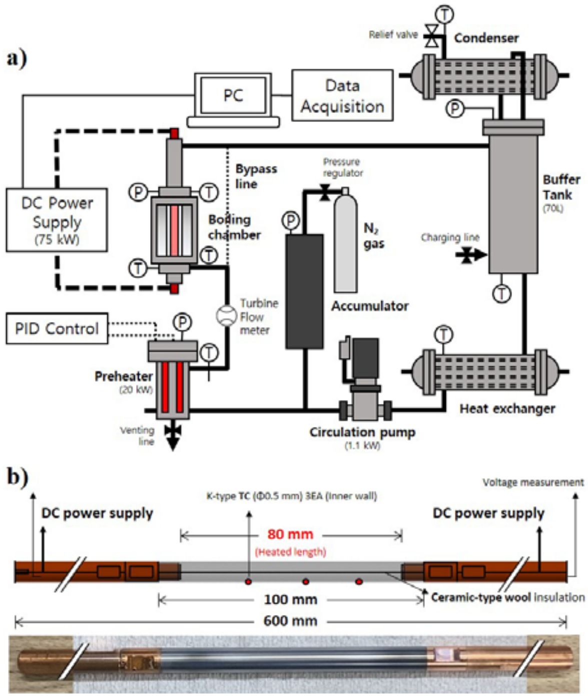

Fig. 2. Schematic diagram of (a) forced convective flow boiling test loop; (b) test section.

Table II: Flow boiling test condition

Test conditions	Characteristics
Test section	Vertical circular tube
Test section material	Zr-based alloy
Outer tube diameter	9.525 mm (3/8 in.)
Heated length	80 mm
Flow type	Annular flow
Outer annular diameter	20 mm
Hydraulic flow diameter	10.475 mm
Loop pressure (MPa)	0.131 (1 atm)
Inlet mass flux (kW/m^{2}s)	400 / 1,500
Subcooled Temp. (^{o}C)	10
Tube	Bare / Cr-coated

The test conditions of conducted flow boiling experiments were listed in Table II. The tests were carried out at a fixed inlet mass flux (400 and 1,500 kg/m^{2}s) and an inlet temperature (90°C) under atmospheric pressure on bare tube and Cr-coated tube. The direct Joule heating method was used to supply the DC power to the test section. This method facilitates stepwise supply of a steady-state heat flux with a control of current input. The DC power input was controlled by a heat flux interval of 100 kW/m^2 and the steady state was determined by observing a steady-state surface temperature maintaining for at least three minutes. The occurrence of CHF was judged to be the point at which the variation in the thermal flux difference over the surface temperature difference increased by more than 1%. The applied heat flux was calculated using the following Joule's heat flux equation:

$$q'' = \frac{Power}{A_{heated}} = \frac{VI}{\pi D L_{heated}} \tag{1}$$

Here, V, I, D, and L_{heated} are the measured voltage drop across the test tube, the measured current, the tube outer diameter, and the heated length, respectively. Uncertainty of the measured heat flux was estimated as 5.2% based on the error propagation method. The maximum heat flux achievable in the test section is about 25 MW/m^2. The heat transfer coefficient, h, was calculated at each measured height as following equation:

$$h = \frac{q''}{T_w - T_{inlet}} \tag{2}$$

Here, T_w and T_{inlet} are the measured wall temperature at each height and chamber inlet temperature, respectively. The heat losses in the test section was calculated by using following normalized difference between the electrical input power and the fluid thermal power.

$$HL(\%) = \frac{VI - \dot{m}c_p(T_{outlet} - T_{inlet})}{VI} \times 100 \tag{3}$$

Here, T_{outlet}, $\dot{m}$, and c_p are the measured chamber outlet temperature, inlet mass flow rate and the average specific heat of liquid between inlet and outlet temperature, respectively. Fig. 3 shows the input power, the fluid thermal power, and the calculated heat loss following experiment time. At high heat flux of interest in CHF experiment, the heat loss is less than 5%.

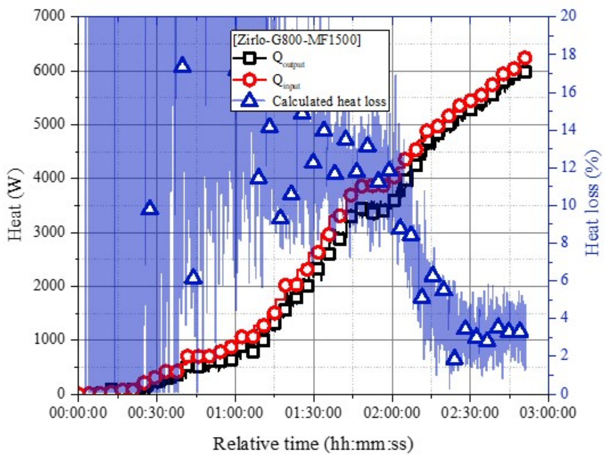

Fig. 3. Comparison of input and output power and calculated heat loss in the test section following the test time.

3. Results and discussion

3.1 Flow boiling CHF experiment results

Fig. 4 shows the boiling curve and heat transfer coefficient of water for tested tubes at the fixed flow conditions as mentioned above. The effect of the coating process on boiling performance (ex) heat transfer coefficient) was not clearly apparent in the single-phase natural convection regime at low heat flux. Instead, the effect of mass flux was evident, with a distinctly high heat transfer coefficient at 1500 kg/m^2s, increasing the slope of the boiling curve. After the point of onset of nucleate boiling (ONB), he overlapping boiling curve shown in the same mass flux case at low heat flux began to differ due to the significantly different vapor generation behavior. At high heat flux, the subcooled flow boiling CHF at the mass flux of 400 kg/m^2s was measured as 1296.8 and 1321.2 kW/m^2 on Zr-based and Cr-coated tubes, respectively. On the other hand, CHF at the mass flux of 1,500 kg/m^2s was measured as 2657.7 and 2534.9 kW/m^2 on Zr-based and Cr-coated tubes, respectively. The enhancement ratio of coating specimens were +1.88% and -4.62% on 400 kg/m^2s and 1,500 kg/m^2s, respectively. Since these enhancement ratios in the CHF were within the error of measurement, it is considered that the CHF increase in each case has not occurred.

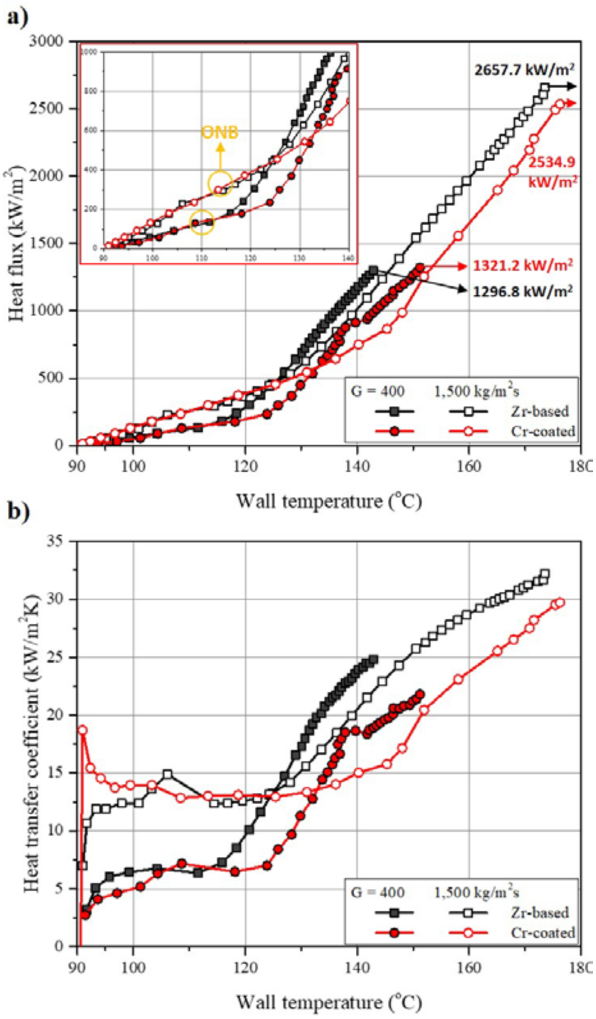

Fig. 5 (a) Boiling curves and (b) heat transfer coefficient of water for tested tubes at the fixed flow conditions (10 ºC inlet subcooling, 0.131 MPa, and 400&1,500 kg/m^2s).

3.2 Variation of coating effect on subcooled flow boiling CHF with Mass flux

As widely known, the nano and microscale surface structures resulting from the coating process of the ATF cladding candidates can enhance the critical heat flux with amplifying the wicking ability on surface in pool boiling condition. However, if there is a liquid flow in the test section, the influence of the surface structures on the CHF become less than pool boiling condition because the wicking force sucked under the vapor is relatively small compared to the force caused by the bulk flow. In order to evaluate the effect of the formation of surface structures on subcooled flow boiling CHF with mass flux, the above results of flow boiling cases were compared with previously performed pool boiling test results on Zr-based and Cr-coated tubes as shown in Fig. 5. The single-phase heat transfer coefficients in pool boiling cases at low heat flux were lower than those in flow boiling cases at both mass flux (400 & 1,500 kg/m^2). The CHF results were also lower than flow boiling cases, which were 751.5 and 1008.0 kW/m^2 on Zr-based and Cr-coated cases, respectively. Fig. 5(b) shows the comparison of

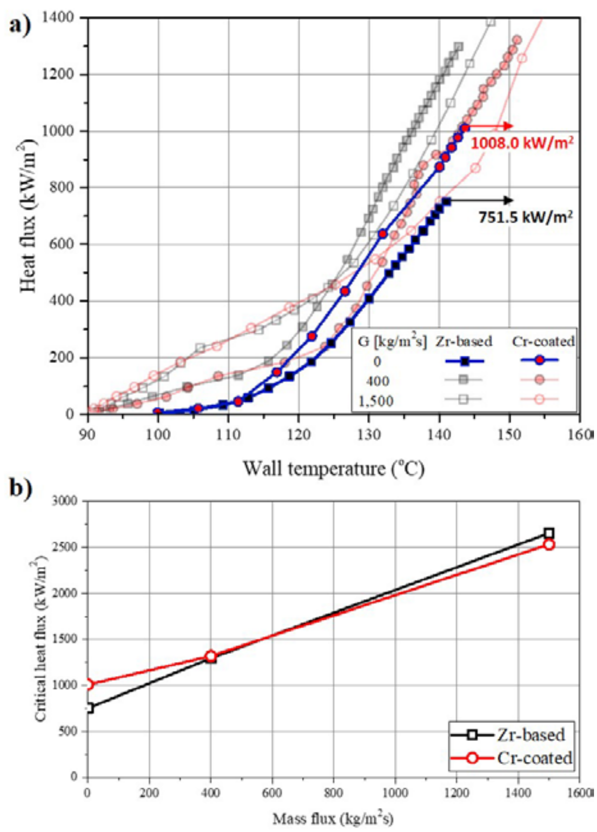

Fig. 4. (a) Boiling curves of Zr-based and Cr-coated tubes at saturated pool boiling condition.; (b) Comparison of measured CHF values following the mass flux condition.

measured CHF values following the mass flux condition. In the pool boiling condition, the CHF of the Cr-coated tube increased to 34% compared to the bare tube, showing the effect of enhancing CHF due to the formation of the surface structure. On the contrary, in the case of flow boiling at a low flow rate (400 kg/m^{2}s) and at a high flow rate of 1500 kg/m^{2}s, CHF showed almost similar values. In terms of this, it was found that the ATF cladding coating process can benefit from the enhance of the CHF in case of an accident such as stationary blackout (SBO) accident, in which the reactor pump stops operating. In the case of subcooled flow boiling condition in the normal operation, however, the gain of the surface structure on the CHF can be reduced.

4. Conclusion

Subcooled flow boiling experiments were conducted with Cr-coated tube by DC magnetron sputtering technique under atmospheric pressure at fixed flow condition of 10 ^{o}C inlet subcooling and 400&1,500 kg/m^{2}s mass flux. It was confirmed that there was no coating effect on boiling heat transfer in the single-phase natural convection regime at low heat flux. In addition, at high heat flux near the CHF, the CHF enhancement effect by the surface structure is significantly affected by the mass flux in test section.

Acknowledgement

This research was supported by the National Research Foundation of Korea (NRF) grant funded by the Korean government (MSIP: Ministry of Science, ICT and Future Planning) (No. NRF-2020M2A8A5025124)

REFERENCES

[1] H.H. Son, Y.S. Cho and S.J. Kim, Experimental study of saturated pool boiling heat transfer with FeCrAl- and Cr-layered vertical tubes under atmospheric pressure, International Journal of Heat and Mass Transfer, Vol.128, p.418–430, 2019.
[2] N. Kim, H.H. Son and S.J. Kim, Oxidation effect on pool boiling critical heat flux enhancement of Cr-coated surface for accident-tolerant fuel cladding application, International Journal of Heat and Mass Transfer, Vol.144, 118655.
[3] J.A. Thornton, Influence of apparatus geometry and deposition conditions on the structure and topography of thick sputtered coatings, Journal of Vacuum Science and Technology. Vol.11, p.666–670, 1974.
[4] K.H. Chu, R. Enright, E.N. Wang, Structured surfaces for enhanced pool boiling heat transfer, Appl. Phys. Lett. 100 (24) (2012) 241603.